UDC 669.245.018.044:620.193.53

Sergiy Byelikov	Dr. Sc., Professor, Professor of the Department of Transport Technologies, National University Zaporizhzhia Polytechnic, Zaporizhzhia, Ukraine, *e-mail: belikov@zp.edu.ua*, ORCID: 0000-0002-9510-8190
Vitaliy Kononov	Candidate of Technical Sciences, Associate Professor of the Department of parts of Machines and Lifting and Transport Mechanisms, National University Zaporizhzhia Polytechnic, Zaporizhzhia, Ukraine, *e-mail: kononov1705@gmail.com*, ORCID: 0000-0002-0479-1386
Olexandr Hlotka	Candidate of Technical Sciences, Associate Professor of the Department of Physical Material Science, National University Zaporizhzhia Polytechnic, Zaporizhzhia, Ukraine, *e-mail: glotka-alexander@ukr.net*, ORCID: 0000- 0002-3117-2687
Michael Sydorenko	Candidate of Technical Sciences, Associate Professor of the Department of parts of Machines and Lifting and Transport Mechanisms, National University Zaporizhzhia Polytechnic, Zaporizhzhia, Ukraine, *e-mail:* s*idorenko.mik@gmail.com*, ORCID: 0000-0002-9097-9739
Sergiy Pychek	Post-graduate student of the Department of Transport Technologies, National University Zaporizhzhia Polytechnic, Zaporizhzhia, Ukraine, *e-mail: puchek777@gmail.com*, ORCID: 0009-0007-8077-6106

COMPARATIVE ANALYSIS OF THE COMPLEX OF PROPERTIES OF NICKEL-BASED SUPERALLOYS

Purpose. *To conduct comparative studies of the complex of physico-mechanical properties of the imported alloy N-155 and the domestic alloy 3MI-11 in order to increase the service life of the rotating blades. To conduct comparative tests on the short-term and long-term strength of the alloys in the initial state (after heat treatment), to conduct comparative tests on the short-term and long-term strength of the alloys after prolonged thermal action at T = 850 ℃, 950 ℃ for 1000, 3000, 5000 hours and to conduct research by metallographic method and micro-X-ray spectral analysis of the microstructure and phase composition of the alloys.*

Research methods. *Alloy samples were made from ingots weighing 10 kg in a vacuum induction furnace УПППФ-3М in an argon environment at a pressure of 1.4–5.3 Pa in crucibles with the main lining with simultaneous pouring of samples of equiaxed crystallization. Chemical analysis was carried out by standard methods in accordance with the requirements of TU 14-1689-73 and OST 1.90127-85. Microstructure studies were carried out on microsections, the plane of which was oriented normal to the surface on a light optical microscope "Olympus IX-70" with a digital video camera "ExwaveHAD color video camera Digital Sony" at magnifications ×200, ×500, ×1000. Strength tests (GOST 1497-61, GOST 9651-61, GOST 1497-84) were carried out on standard cylindrical samples (diameter of the working part 5 mm, length 25 mm) at temperatures 200, 800, 900 and 1000℃ on a УМЕ-10ТМ brand tensile machine. Long-term strength tests (GOST 10145-81) were carried out on standard cylindrical samples at temperatures 800, 900, 10000 ℃ and corresponding loads 600, 400, 180 MPa on an AIMA-5-2 machine.*

Obtained results. *It was found that during tests at 800 and 900℃, the tensile strength of the N-155 alloy is 1.2 times lower than that of 3MI-11, and the long-term strength is 5.2 times lower, respectively. It was shown that the amount of the strengthening phase in the 3MI-11 alloy is 6…10 % more, evenly distributed throughout the alloy body. It was established that in the composition of the strengthening phase of the 3MI-11 alloy, the concentration of chromium, tungsten, and molybdenum remains practically unchanged and does not depend on the presence of niobium. At the same time, in the composition of the strengthening phase of the 3MI-11 alloy, the concentration of cobalt increases by 1.4 times, and the concentration of aluminum and titanium decreases by 1.1 times compared to the N-155 alloy. It was established that in the process of dissolving non-equilibrium eutectic precipitates, microvolumes arise, locally supersaturated with tungsten, chromium, and titanium, in which the probability of the formation of carbides on a more complex basis increases. It was found that during prolonged thermal action carbides based on tantalum TaC and on a mixed basis (Ta, Ti) C in the 3MI-11 alloy are thermally more stable than carbides in the N-155 alloy.*

Scientific novelty. *The obtained results allow us to understand the thermodynamics of phase formation processes in two alloying systems and to establish the relationships between alloying elements concentration and the phase composition of the alloy.*

Practical value. *The obtained results allow us to recommend the domestic 3MI-11 as a substitute for the foreign alloy N-155 without loss of properties and service life.*

Key words: *nickel-based superalloys, phase composition, distribution of alloying elements, heat resistance, carbides.*

DOI 10.15588/1607-6885-2025-1-2

Introduction

Today, there is a need to obtain products with a high level of physical, mechanical and operational properties of modern heat-resistant nickel alloys. This can be achieved by quite complex alloying systems [1–5]. There are quite effective ways to improve a number of properties of existing alloys, such as modification and other technological methods that allow improving the structure and quality of the material of the final product [4–6]. However, it is possible to influence the properties by changing the chemical composition of structural components without significantly changing the composition of the alloy. For example, it has been shown that changing the chemical composition of carbides leads to a change in their shape, size and melting temperature [7–10]. As a result, the operational characteristics of experimental compositions improve.

Purpose of the work

To conduct comparative studies of the complex of physico-mechanical properties of the imported alloy N-155 and the domestic alloy ЗМІ-11 in order to increase the service life of rotating blades.

Material and research methods

The solution to the tasks is possible only with a comprehensive approach to studying the structure and properties of the alloy ЗМІ-11 in comparison with the alloy N-155 before and after prolonged thermal action at operating temperatures on strength characteristics, structural and phase stability. Comparison of research results makes it possible to predict the long-term strength and structural stability of the alloy ЗМІ-11 in order to increase the service life of rotating TNT blades, which is relevant for parts of stationary gas turbines.

Samples of alloys N-155 and ЗМІ-11 were manufactured by obtaining ingots weighing 10 kg in a vacuum induction furnace УППФ-3М in an argon environment at a pressure of 1.4–5.3 Pa in crucibles with the main lining with simultaneous pouring of samples of equiaxed crystallization. Metal casting was done in ceramic molds, preheated to 9000 °C at a metal temperature of 15400 °C. Then the cast blanks were heat treated in vacuum or neutral atmosphere according to the specified regime, after which standard cylindrical samples were manufactured for mechanical tests.

Further, comparative studies of mechanical properties, microstructure and phase composition of alloys were carried out. The nominal chemical composition of the alloys is given in Table 1.

Chemical analysis of alloys N-155 and ЗМІ-11 was carried out by standard methods in accordance with the requirements of TU 14-1689-73 and OST 1.90127-85. Spectral chemical analysis was carried out on an optical emission device ARL-4460 (quantometer for simultaneous multi-channel analysis of elements). Wavelength range from 170 nm to 800 nm.

Table 1 – Chemical composition of alloys

Alloy	Element content % (by mass)											
	C	Cr	Al	Ti	Mo	W	Co	Nb	B	Zr	N_2	Ni
N-155	0,15	21,0	-	-	3,0	2,5	20,0	1,0	-	-	0,15	ост.
ЗМІ-11	0,125	16,0	1,25	1,75	2,0	3,0	-	1,0	0,01	0,01	-	ост.

The microstructure of the samples was studied on unetched and etched microsections, the plane of which was oriented normal to the surface on a light optical microscope “Olympus IX–70” with a digital video camera “ExwaveHAD color video camera Digital Sony” at magnifications of ×200, ×500, ×1000. The microstructure was detected by etching the surfaces of the sections with Marble's reagent – $CuSO_4$ – 4 g, HCl – 20 ml, water – 20 ml according to the following regimen: etching for 10–15 seconds, rinsing with water, drying with hot air.

To detect the γ′-phase, the reagent $CuSO_4$ – 20 g, H_2SO_4 – 5 ml, the rest H_2O, current density – 500 A/m^2.

To detect carbides, boride, nitride, the reagent NaF – 30 g, HCl – 100 ml, citric acid – 100 g, H_2O – 1000 ml, current density – 200 A/m^2 was used.

To identify the σ – phase and carbides of the M_6C type, which have a similar needle morphology, they are etched using the reagent: red blood salt – 10 g, NaOH – 10 g, H_2O – 100 ml, current density 500 A/m^2. In this case, the σ – phase was colored brown, and the double carbides were colored black. The study of the fine structure (morphology and phase composition) of alloys N-155 and ЗМІ-11 after casting, heat treatment and long-term aging at T = 8500 and 950 °C for 1000, 3000, 5000 hours was studied by electron microscopy on a JEOL JSM – 6360la scanning microscope at magnifications of ×5000, ×10000.

The sizes, shape and number of γ′- q`phase particles were determined by electron microscopy on replicas. The size of the γ′-p hase was estimated on cross sections at magnification of ×10000. Measurements were made on one side of the cube. Quantitative metallography was used to calculate the volumetric content of the γ′- phase, γ-γ′ eutectic, and carbide phase in the tested alloys.

Short-term strength tests (GOST 1497-61, GOST 9651-61, GOST 1497-84) were performed on standard cylindrical samples (diameter of the working part 5 mm, length 25 mm) at temperatures of 200, 800, 900 and 10000 °C on a UME-10TM brand tensile machine. Long-term strength tests (GOST 10145-81) were performed on standard cylindrical samples at temperatures of 800, 900, 10000 °C and corresponding loads of 600, 400, 180 MPa on an AIMA-5-2 machine by uniaxial stretching of samples under constant load. The relative elongation of the samples was recorded using mechanical strain gauges. At each load level, 3–5 samples were tested.

To assess the degree of reduction in the strength characteristics of the studied alloys as a result of prolonged thermal action at temperatures of 8500 and 950 °C with different aging bases of 1000, 3000, 5000 hours, additional tests of samples were carried out in accordance with the above-mentioned standards.

To identify the phases in the alloys, the method of local microprobe analysis was used. The accelerating voltage was 10 keV, the diameter of the electron probe was 4 nm (40AO). The study of the chemical composition of the phases was carried out on the X- ray spectral analysis attachment to the JEOL JSM-6360la scanning electron microscope with the JED-2300 energy-dispersive X-ray spectral microanalysis system. Using this method, changes in the morphology and composition of the γ′-

DOI 10.15588/1607-6885-2025-1-2

phase, γ-γ′ eutectic, and carbide phase before and after prolonged thermal action were studied.

Research results and their discussion

In order to form an optimal structure to ensure a complex of mechanical properties, heat treatment (HT) of alloys N-155 and 3MI-11 was carried out in a 2-s tage mode. As mentioned above, the homogenization temperature (I-th stage of heat treatment) for each alloy was assigned individually based on the analysis of data obtained by the method of differential thermal analysis (DTA). Table 2 presents the heat treatment modes for the alloys.

Table 2 – Heat treatment modes of alloys

Alloy	$T_{гом.}$, °C	$T_{ст.}$, °C	Exposure time, between steps, h	Cooling rate, between steps, °/min
N-155	1180	1050	4	in the air
3MI-11	1240	1050	4	in the air

High-temperature aging (II degree of TO) of alloys was carried out at a temperature of 10500 °C, which was chosen close to the technological temperature of applying the protective coating.

Comparative analysis of the results of Table 3 showed that at test temperatures of 8000 and 9000 °C, the tensile strength σ_B of the N-155 alloy is 1.2 times lower than that of the 3MI-11 alloy. The yield strength $\sigma_{0.2}$ of the N-155 alloy is 1.3 times lower than that of the 3MI-11 alloy. At a test temperature of 1000 °C, the tensile strength of the N-155 alloy is 1.4 times lower than that of the 3MI-11 alloy. The yield strength of the N-155 alloy is 1.5 times lower than that of the 3MI-11 alloy. At the same time, the N-155 alloy has higher plasticity. Comparative analysis of the data of Table 4 showed that at all test temperatures, the durability of the N-155 alloy is significantly lower than that of the 3MI-11 alloy under equal test conditions.

Table 3 – Short-term strength of alloys in the initial state (after HT)

Alloys	$T_{вип.}$, °C	σ_B, МПа	$\sigma_{0.2}$, MPa	δ, %	ψ, %
N-155	800	990	805	9,6	22,2
	900	620	470	19,1	31,3
	1000	340	180	21,3	42,2
3MI-11	800	1070	950	7,8	17,1
	900	720	630	13,4	25,6
	1000	490	300	17,0	33,3

Table 4 – Long-term strength of alloys

Alloy	$T_{ВИП.,.}$ °C	σ, MPa	τ, hour	δ, %	ψ, %
N-155	800	450	154,2	11,1	22,2
N-155	900	250	137,9	13,9	31,3
N-155	1000	120	115,5	16,6	46,3
3MI-11	800	450	801,7	9,8	18,0
3MI-11	900	250	748,1	14,1	25,4
3MI-11	1000	120	782,0	12,1	29,8

Thus, at a test temperature of 800 °C and a stress of 450 MPa, the time to fracture of samples of alloy N-155 is 5.2 times less than that of alloy 3MI-11. At a test temperature of 9000C and a stress of 250 MPa, the time to fracture of samples of alloy N-155 is 5.4 times less than that of alloy 3MI-11. At a test temperature of 10000C and a stress of 120 MPa, the time to fracture of samples of alloy N-155 is 6.8 times less than that of alloy 3MI-11. At the same time, the plasticity of alloy 3MI-11 is slightly lower compared to alloy N-155. The results obtained after prolonged thermal action at 850 °C on all time bases showed that at test temperatures of 800, 900, 1000 °C, the properties of alloys decrease by different at the same rate under the same test conditions, compared with the initial properties (after HT). At the same time, the decrease in the heat resistance of the alloy N-155 occurs more intensively than in the alloy 3MI- 11 at all time bases of aging.

Thus, in the alloy N-155 after aging at 850 °C for 5000 hours, the ultimate strength at the test temperature of 8000 °C decreases by 40–45 MPa, at 900 °C by 55–60 MPa, at 1000 °C by 95–100 MPa.

The plasticity remains at the initial level. At the same time, the ultimate strength of the alloy 3MI- 11 decreases less intensively. After prolonged aging at 850°C for 5000 hours in the alloy 3MI-11, the ultimate strength at test temperatures of 8000 and 900 °C decreases by 35–40 MPa, at 1000 °C by 55–60 MPa compared to the initial state. At the same time, compared to the alloy N-155, a slight decrease in plasticity is observed in the alloy 3MI-11. The results obtained after prolonged thermal action at 9500C on all time bases showed that at test temperatures of 800, 900, 1000 °C the properties of the alloys decrease at a more intensive rate under equal test conditions, compared to the initial properties (after HT). At the same time, the rate of decrease in the heat resistance of the alloy N-155 occurs significantly more intensively than in the alloy 3MI-11 on all time bases of aging.

In alloy N-155 after aging at 950 °C for 5000 hours, the ultimate strength at the test temperature of 800 °C decreases by 60-65 MPa, at 900 °C by 75–80 MPa, at 1000 °C by 130–135 MPa.

The ductility decreases by 4–6 % compared to the initial state at all test temperatures. At the same time, the ultimate strength of alloy 3MI-11 decreases less intensively.

In alloy 3MI-11, the ultimate strength after prolonged aging at 950 °C for 5000 hours at test temperatures of 8000 and 900 °C decreases by 45–55 MPa, at 1000 °C by 75–80 MPa compared to the initial state. At the same time, a significant difference in the tensile strength of the alloy N-155 and 3MI-11 is observed at a test temperature of 1000 °C.

It was established that in the 3MI-11 alloy there is a decrease in plasticity by an average of 5–7 % compared to the initial state (after HT) at all test temperatures.

Metallographic studies have shown that in the cast state the structure of the alloys is heterophase with a pronounced dendritic character, which is manifested in the uneven distribution of particles of the γ′- phase, the γ-γ′ eutectic and the carbide phase (Fig. 1).

DOI 10.15588/1607-6885-2025-1-2

a ×200 *b* ×200

Figure 1. Dendritic structure of alloys after casting: *a* – alloy – N-155; *b* – alloy – 3MI-11

It was found that in comparison with the N-155 alloy, the volume fraction of the strengthening phase in the 3MI-11 alloy increases by 6.0–8.0 %, and the eutectic phase by 2.5–3.5 %. At the same time, the amount of the main strengthening phase in the N-155 alloy is 48–50 %, in the 3MI-11 alloy it is 56–58 %. After crystallization, the formation of carbides of the MeC type is observed in the structure of the alloys near large eutectic precipitates, which partially fill the space between the dendrite branches (Fig. 1). Comparative studies have shown that the carbide phase in the N-155 alloy is mainly located in localized interdendritic areas in the form of "skeletal" precipitates in the form of the so-called "Chinese characters".

The carbide phase in the alloy 3MI-11 has a morphology in the form of individual polygonal and discontinuous inclusions of irregular spherical shape. The electron micrographs (Fig. 2) illustrate the morphology and arrangement of phases after casting in the structure of alloys N-155 and 3MI-11. It should be noted that the distribution density, size and shape of γ- phase particles in the interdendritic areas and dendrite axes are different. Thus, together with fine particles of γ- phase, large eutectic precipitates of γ - phase are observed, which were formed at the final stage of crystallization in the interaxial dendritic spaces.

Metallographic analysis of the structure and X-ray spectral microanalysis data showed that during crystallization the interdendritic melt is enriched with γ′-forming elements, which leads to an increased size of precipitates of γ'_{eut}.- phase of eutectic origin in the interaxial areas.

In the center of the axes of the I-th order dendrite, the γ-phase is isolated in the form of cubic particles with a size of 0.30–0.40 μm, in the interdendritic region - in the form of irregular subcubes with a size of 0.8–1.5 μm and more. It was established that in the structure of the 3MI - 11 alloy, in comparison with N-155, the morphology of the eutectic precipitates changes.

In the N-155 alloy, the eutectic precipitates have a characteristic fan-shaped shape and are a bundle of diverging γ-phase particles separated by thin veins of the γ-solid solution (Fig. 2*a*), in the 3MI-11 alloy, the eutectic precipitates have a morphology from faceted to lamellar (Fig. 2*b*).

The X-ray spectral microanalysis data showed that both polygonal and skeletal precipitates are carbides of the MiC type. At the same time, the morphology of the carbide phase shows that polygonal carbides are formed near liquidus temperatures, and skeletal carbides as a result of the eutectic reaction. Thus, in alloys N - 155 and 3MI-11 carbides on the bases of TiC, (Ti, Nb) C, growing in the melt, have a block-like shape with regular faceting (Fig. 2).

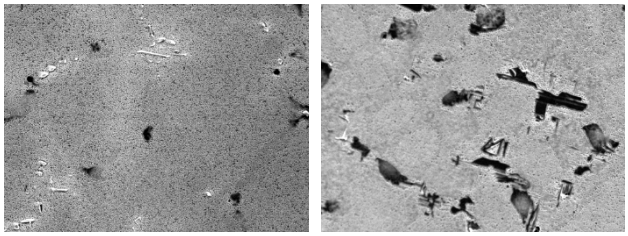

a ×500 *b* ×500

Figure 2. Distribution and morphology of phases in the microstructure of alloys after casting: *a* – alloy N-155; *b* – alloy 3MI-11

Fig. 3 shows the distribution of the main strengthening phase in the microstructure of alloys N-155 and 3MI-11 after casting. Metallographic analysis showed that after crystallization, the particles of the main strengthening phase were fairly evenly separated in the matrix and have a shape from cubic to rectangular.

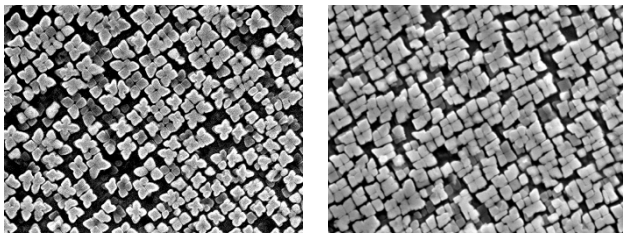

a ×10 000 *b* ×10 000

Figure 3. Distribution of the strengthening phase in the microstructure of alloys after casting: *a* – alloy – N-155; *b* – alloy – 3MI-11

At the same time, the most ordered and dense distribution of cubic particles of the main strengthening phase with a uniform distance between them is observed in the microstructure of the alloys (Fig. 3). The average size of the particles of the strengthening phase is on average 0.40–0.50 microns. It should be noted that in the cast state, the cubic morphology of the strengthening phase in the alloys indicates the tension and non-equilibrium of the structure.

Fig. 4 shows the distribution of the main strengthening phase in the microstructure of alloys N-155 and 3MI-11 after heat treatment.

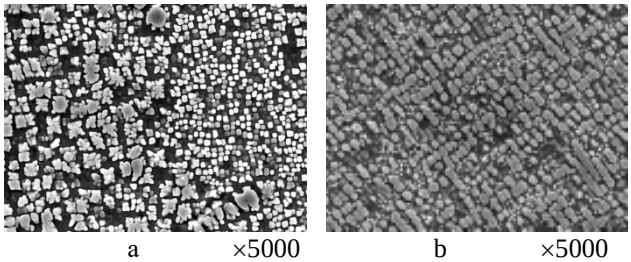

a ×5000 b ×5000

Figure .4 Distribution of the strengthening phase in the structure of alloys after HT: *a* – alloy – N-155; *b* – alloy – 3MI-11

DOI 10.15588/1607-6885-2025-1-2

After high-temperature aging at 1050 °C (II-th degree of HT) in the structure of alloys, coagulation of particles of the strengthening phase that have not dissolved is observed, in connection with which, along with fine particles, larger particles of the phase are also observed. When cooling in air, the maximum possible volume fraction of the strengthening phase is achieved in alloys.

It has been established that in the process of high-temperature aging (II-th degree of HT) particles of the strengthening phase lose the correct cubic shape. In the fully heat-treated state, the structure of the alloys is bimodal.

At the same time, the particles of the larger fraction of the formed rounded shape, with a size of 0.70–0.90 μm and the particles of the strengthening phase of the fine-dispersed fraction with a size of 0.20–0.30 μm, are fairly evenly distributed in the matrix. The average size of the particles of the strengthening phase in the alloy structure is 0.50–0.70 μm.

Fig. 5 shows the distribution of phases in the microstructure of alloys N-155 and 3MI-11 after high-temperature aging at T = 1050 °C.

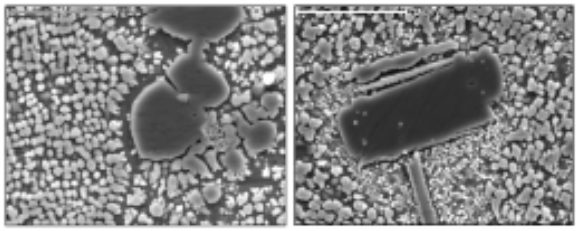

a ×5000 *b* ×5000

Figure 5. Distribution of phases in the microstructure of alloys after HT:
a – strengthening phase and eutectic in alloy N-155;
b – strengthening phase and eutectic in alloy 3MI-11

As can be seen in Fig. 5, the eutectic precipitates did not completely dissolve due to the lower homogenization temperature and short holding time, which was associated with the risk of eutectic melting and could lead to increased microstructural heterogeneity.

After heat treatment, the eutectic precipitates remain in the places of their preferential separation during crystallization. At the same time, zones are formed around them where the secondary separations of the strengthening phase are much more dispersed than in other areas of the matrix. It is characteristic that in these areas particles of the strengthening phase of the fine-dispersed fraction with a size of 0.15–0.20 μm and less are observed.

Fine-dispersed particles are further separated during high-temperature aging as a result of the decay of the supersaturated solid solution due to the concentration heterogeneity of the elements. After heat treatment, the carbide phase in the alloys does not undergo noticeable changes. Thus, in the process of 2- stage heat treatment in the alloys formed an optimal, equilibrium and stable structure. At the same time, the total number of non-equilibrium phases is noticeably reduced. The optimal distribution of strengthening phases in the structure of the alloys corresponds to more stable values of short-term and long-term strength, which is confirmed by mechanical tests.

The chemical composition of the phases is determined by the initial chemical composition of the alloy. At the same time, the determination of the chemical composition of the phases by elements requires accurate quantitative analysis within the phase.

Therefore, the dependence between the composition of the alloys N-155, 3MI-11 and their chemical composition of the phases was investigated. Analysis of Xray spectral microanalysis data showed, and mechanical tests confirmed, that the increase in short-term and long-term strength of the 3MI-11 alloy, compared with the N-155 alloy, is more related not so much to the increase in the volume fraction of the main strengthening phase, but to a change in its chemical composition.

Depending on the conditions of dendrite formation, the main strengthening phase has a noticeable difference in chemical composition compared with the phases of eutectic origin. Moreover, a noticeable difference in the chemical composition of the phases is observed for the most strongly liquifying elements. Thus, the eutectic, compared with the main strengthening phase, is enriched in elements whose liquification coefficient is positive (aluminum, titanium), and depleted in elements whose liquification coefficient is negative (chromium, cobalt, tungsten).

In Fig. 6 shows large eutectic precipitates in the interdendritic spaces, which have a noticeable heterogeneity in the distribution of alloying elements in alloys N- 155 and 3MI-11.

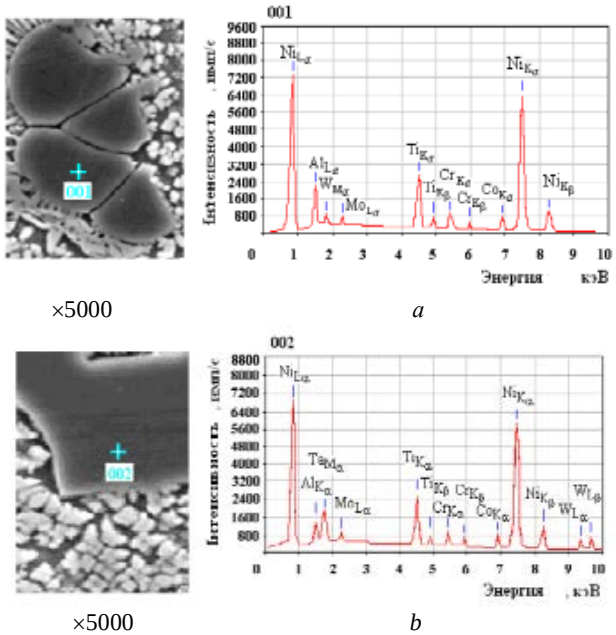

×5000 *a*

×5000 *b*

Figure 6. Chemical composition of the eutectic:
a – alloy N-155; *b* – alloy 3MI-11

The liquation nature of the distribution of elements participating in the formation of the eutectic phase leads to its uneven separation in the volume of the alloy. In the interdendritic areas, supersaturated with aluminum and titanium, the eutectic phase is separated in large sizes due

DOI 10.15588/1607-6885-2025-1-2

to the fact that these elements have the greatest liquation and are included in it, as the main ones, together with aluminum.

Using electron microscopy, it was established that the eutectic phase of the 3MI-11 alloy, separated in the interdendritic areas, differs in both chemical composition and morphology in comparison with the N-155 alloy. Thus, in the 3MI-11 alloy, alloying with aluminum and titanium leads to an increase in the volume fraction of eutectic separations by 2.5–3.5%. In the interdendritic regions, the strengthening phase is 3-5 times larger than in the center of the dendrite axes. Table 4 shows the comparative results of the quantitative analysis of the chemical composition of the eutectic phase of the alloys, obtained using the electron microprobe method X-ray spectral microanalysis.

Table 4 – Chemical composition of eutectic alloys

Alloy	Content of elements in eutectic, % (by mass)							
	Cr	Co	W	Mo	Al	Ti	Nb	Ni
N-155	2,8	2,3	3,6	0,2	-	-	6,9	75,4
3MI-11	2,6	-	2,9	0,1	5,4	8,1	6,9	71,6

Metallographic studies and X-ray spectral microanalysis data showed that in the interdendritic layers the eutectic phase differs in composition from the main strengthening phase. At the same time, both small and large areas of eutectic precipitates are enriched in aluminum, titanium, and depleted in tungsten, molybdenum, chromium, cobalt in comparison with the solid solution. Thus, in the composition of the eutectic of the 3MI-11 alloy, the concentration of chromium, cobalt and molybdenum remains constant and does not depend on the concentration of titanium in the alloy. In the composition of the eutectic phase of the 3MI-11 alloy, the amount of tungsten and aluminum decreases by 1.3 times, and the concentration of titanium by 1.1 times in comparison with the N-155 alloy. At the same time, in the composition of the eutectic phase, the concentration of chromium is 4.5–5 times lower, cobalt, tungsten and molybdenum is 2.5–3 times lower, and the concentration of aluminum and titanium is 1.7–2 times higher than their concentration in the main composition of the alloy. At the same time, with the presence of titanium in the composition of the eutectic phase of the alloy 3MI-11, the temperature of eutectic t_{eut}. transformations increases by 500 °C, and therefore, the thermal stability of eutectic precipitates increases in comparison with the alloy N-155.

Fig. 7 shows the chemical composition of the strengthening phase of alloys N-155 and 3MI-11. Using electron microscopy and the X-ray spectral microanalysis method, it was found that with the presence of aluminum and titanium in the composition of the 3MI-11 alloy, the composition of the strengthening phase changes compared to the N-155 alloy.

Table 5 shows the results of quantitative analysis of the chemical composition of the main strengthening phase of alloys N-155 and 3MI-11, obtained using an electron microprobe. It was found that in the composition of the strengthening phase of the 3MI-11 alloy, the concentration of chromium, tungsten and molybdenum remains practically unchanged and does not depend on the presence of niobium. At the same time, in the composition of the strengthening phase of the 3MI-11 alloy, the concentration of cobalt increases by 1.4 times, and the concentration of aluminum and titanium decreases by 1.1 times compared to the N-155 alloy.

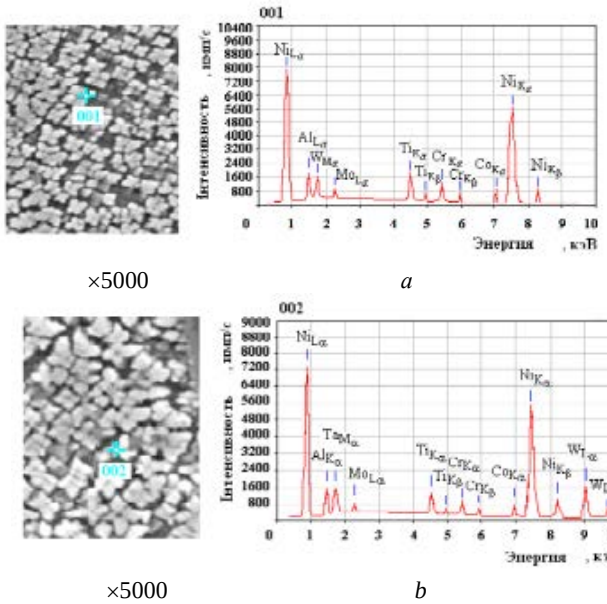

Figure 7. Chemical composition of the main strengthening phase: *a* – alloy N-155; *b* – alloy 3MI-11

Table 5 – Chemical composition of the strengthening phase of alloys

Alloy	Content of elements in the strengthening phase, % (by mass)							
	Cr	Co	W	Mo	Al	Ti	Ta	Ni
N-155	2,9	2,5	7,1	0,4	--	7,4	--	72,5
3MI-11	2,7	3,3	6,9	0,2	6,6	6,9	5,7	67,7

It should be noted that in the alloy 3MI-11 aluminum, titanium, tungsten in the strengthening phase are approximately in the same concentration. Thus, in comparison with the alloy N-155, where the main strengthening phases are carbides and nitrides, in the alloy 3MI-11, which showed higher short-term and long-term strength, in the composition of the strengthening phase part of aluminum and titanium is replaced by the most optimal ratio of refractory elements – tantalum and tungsten (table 5). Therefore, the main strengthening phase of the alloy 3MI-11 at 70–750 °C has a higher temperature of the end of dissolution of t_{ed}, in comparison with the alloy N-155, and therefore, higher thermal stability.

According to microanalysis data, the concentration of chromium in the composition of the strengthening phase of the alloys is 4.5-5 times, and cobalt and molybdenum 1.5 - 2 times lower than their concentration in the main composition. At the same time, the concentration of tungsten in the strengthening phase is practically the same as in the main composition. At the

DOI 10.15588/1607-6885-2025-1-2

same time, the concentration of aluminum is 1.7–2 times, and titanium and tantalum 1.3–1.4 times higher than their concentration in the main composition of the alloys. Thus, a comparative analysis of the results given in Tables 5 and 6 showed that in comparison with the N-155 alloy, in the 3MI-11 alloy aluminum and titanium in the composition of the eutectic and strengthening phase are replaced by more refractory tantalum, the content of which reaches: in the eutectic 7–8 %, in the strengthening phase 6–7 %.

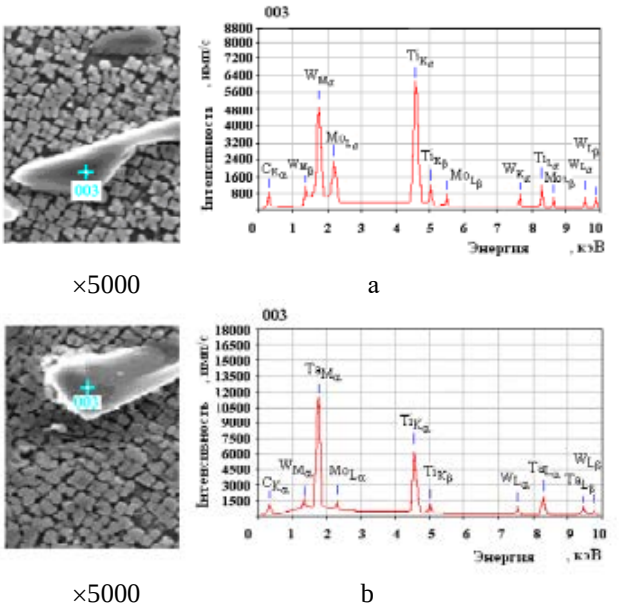

Figure 8 - Chemical composition of carbide type MeC: a - alloy N-155; b - alloy 3MI-11.

Fig. 8 presents the results of a comparative study of the chemical composition of the carbide phase of the MeC type of alloys N - 155 and 3MI-11. Data analysis showed that in the cast state, carbides based on TiC (Fig. 8 a) containing a high concentration of tungsten are observed in the alloy N - 155. In the alloy 3MI-11, carbides are observed mainly on a mixed basis (Ti, Ta) C. The presence of other carbide-forming elements (Ti, W, Mo) allows us to conclude that carbides based on titanium and tantalum are inclusions with complex chemical composition.

Table 6 presents the results of quantitative analysis of the chemical composition of the carbide phase of the alloys, obtained by the X-ray spectral microanalysis method using an electron microprobe. It was found that the presence of titanium in the 3MI-11 alloy has a significant effect on the redistribution of alloying elements in the carbide phase compared to the N-155 alloy.

Analysis of the obtained results in Table 6 showed that the carbide phase in the N - 155 alloy contains up to 37% tungsten and up to 4% molybdenum. In the 3MI-11 alloy, carbides contain the following elements: 56% tantalum; 30% titanium, 13% tungsten and 1% molybdenum. It was found that the presence of tantalum up to 4% in the 3MI-11 alloy leads to an increase in its concentration in the carbide phase to 56 %, which is 12 times higher than its concentration in the main composition. At the same time, in comparison with the N-155 alloy, in the 3MI-11 alloy there is a simultaneous decrease in the titanium concentration by 2.2 times and the total concentration of tungsten and molybdenum by 3.4 times.

At the same time, the presence of titanium in the strengthening phases of the 3MI-11 alloy has a positive effect on the overall strengthening mechanism.

It is known that for alloy N-155 the operating temperature range is 800–850°C. Comparative studies of the complex of mechanical properties have shown that alloy 3MI-11 has higher short-term and long-term strength, compared to alloy N-155, has a temperature capability 500 °C higher and its operating range is 900–950 °C.

Table 6 – Chemical composition of the carbide phase of the alloys

Alloy	Content of elements in the carbide phase, % (by mass)			
	Ti	Ta	W	Mo
N-155	-	-	37	4
3MI-11	30	56	13	1

In this regard, comparative studies of the kinetics of structural transformations in alloys N-155 and 3MI-11 were carried out during prolonged thermal action at temperatures of 850 and 950 °C on the basis of 1000, 3000, 5000 hours. For a comparative assessment of structural and phase stability, the structure formed in the alloys after heat treatment was considered the initial one.

Comparative metallographic analysis of the initial structure showed that the amount of the strengthening phase in the alloy 3MI-11 is 6–8 % more, and the proportion of the phase of eutectic origin is 2.5–3.5 % more than in the structure of the alloy N-155.

X-ray spectral microanalysis showed that the chemical composition of the phases of the alloys is not the same. With the presence of titanium in the alloy 3MI-11, its concentration in the phases increases, in particular, in the strengthening phase. This causes its higher thermal stability at elevated temperatures.

Fig. 9 shows the kinetics of changes in the morphology of the strengthening phase in alloys N-155 and 3MI-11 after prolonged aging at a temperature of 850 °C on time bases of 1000, 3000 and 5000 hours.

Comparative studies of the microstructure showed that after prolonged aging at a temperature of 8500 °C on all time bases in the alloys N-155 and 3MI-11 there is no noticeable difference in the rate of change in the morphology and size of the particles of the strengthening phase (Fig. 9). In the structure of the alloys N-155 and 3MI-11 on the basis of 5000 hours, the initial cubic morphology changes to a spherical irregular shape. No coagulation processes are observed, the distance between the particles remains uniform, and the distribution is ordered. At the same time, metallographic analysis showed that during prolonged thermal action at 8500 °C in the structure of the alloys N-155 and 3MI-11, the processes of dissolution of eutectic precipitates occur on all time bases (Fig. 10).

DOI 10.15588/1607-6885-2025-1-2

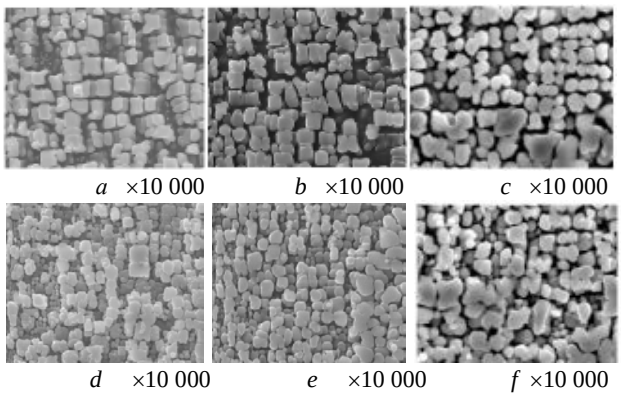

Figure 9. Kinetics of changes in the morphology of the strengthening phase during prolonged thermal action at 8500 °C: *a*, *b*, *c* – alloy N-155 – 1000, 3000, 5000 hours; *d*, *e*, *f* – alloy 3MI-11 – 1000, 3000, 5000 hours.

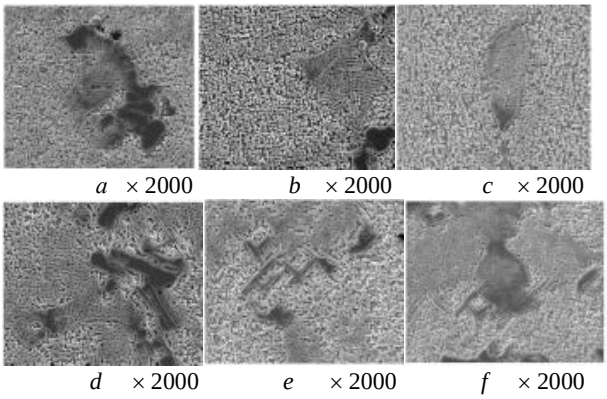

Figure 10. Dissolution of eutectics in alloys during prolonged thermal action at 850 °C: *a*, *b*, *c* – alloy N-155 – 1000, 3000, 5000 hours; *d*, *e*, *f* – alloy 3MI-11 – 1000, 3000, 5000 hours

It was found that during prolonged thermal action, non-equilibrium eutectic precipitates are noticeably dissolved, unlike the strengthening phase. The reason for these transformations is probably the presence of chemical heterogeneity in the alloy structure, due to dendritic liquation, which is a heredity of the cast structure.

In Fig. 11 shows the kinetics of structural changes in the strengthening phase of alloys N-155 and 3MI-11 during long-term thermal aging at a temperature of 950 °C on time bases of 1000, 3000 and 5000 hours. Metallographic analysis showed that the different rate of coagulation of particles of the strengthening phase in alloys N-155 and 3MI-11 can be explained by the different chemical composition and its volume content in the initial state of the alloys.

Comparative studies of the microstructure showed that during prolonged thermal action at 950 °C in alloys N-155 and 3MI-11 there is a noticeable difference in the rate of change in the morphology and particle size of the strengthening phase. The analysis showed that in the microstructure of alloy N-155 there is a more intense increase in the average particle size of the strengthening phase, which is probably due to their growth due to more finely dispersed precipitates. It was found that in the alloy N-155, in comparison with the alloy 3MI-11, the coagulation process and the loss of the correct geometric shape by the particles proceeds more intensively on all time bases (Fig. 11). The initial cubic morphology changes to a spherical irregular shape in the alloy N-155. At the same time, the distance between the particles becomes uneven, and the distribution is chaotic. Such structural changes lead to an acceleration of the rate of decrease in strength characteristics. Such degradation of the structure is caused by more intensive diffusion processes in comparison with the thermal effect at 850 °C. The significant decrease in the coagulation rate of the particles of the strengthening phase in the alloy 3MI-11 in comparison with the alloy N-155, observed by electron microscopy, can be explained by the slowdown in the diffusion mobility of the main elements, those that make up the strengthening phase, in the presence of titanium in its chemical composition.

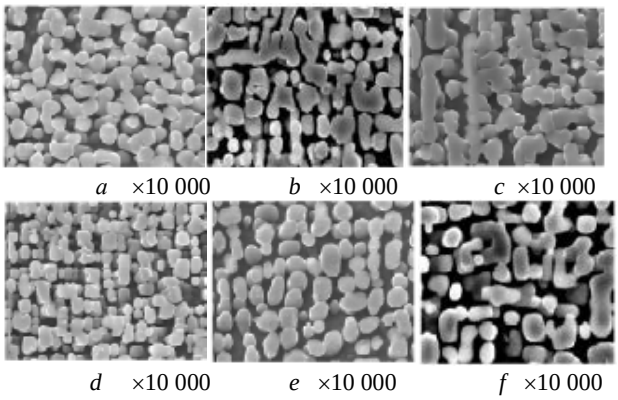

Figure 11. Kinetics of changes in the morphology of the strengthening phase during prolonged thermal action at 9500 °C: *a*, *b*, *c* – alloy N-155 – 1000, 3000, 5000 hours; *d*, *e*, *f* – alloy 3MI-11 – 1000, 3000, 5000 hours

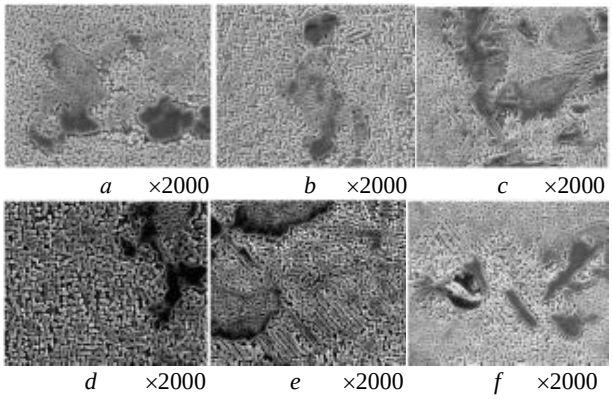

Figure 12. Dissolution of eutectics during prolonged thermal action at 9500 °C: *a*, *b*, *c* – alloy N-155 – 1000, 3000, 5000 hours; *d*, *e*, *f* – alloy ZMI-11 – 1000, 3000, 5000 hours

At the same time, metallographic analysis showed that during prolonged thermal action at 950 °C, more intense processes of dissolution of eutectic precipitates are observed in the structure of alloy N - 155 compared to alloy 3MI-11, between at 850 °C (Fig. 12). The reason for the increase in the intensity of these transformations is probably associated with an increase in the rate of diffusion processes in non-equilibrium phases, due to dendritic liquation, which is a heredity of the cast structure.

DOI 10.15588/1607-6885-2025-1-2

It was established that in the process of dissolution of non-equilibrium eutectic precipitates, microvolumes arise, locally supersaturated with tungsten, chromium, titanium, in which the probability of formation of carbides on a more complex basis increases. In the course of research, it was established that in the process of prolonged thermal action, carbides on the basis of tantalum TaC and on a mixed basis (Ta, Ti) C in the alloy ЗМІ-11 are thermally more stable than carbides in the alloy N-155.

Metallographic analysis showed that, probably, striving for an equilibrium state, there is a gradual alignment of the chemical composition of eutectic precipitates with the composition of the strengthening phase and solid solution. In the process of phase transformations with the participation of coarse eutectic precipitates in alloys, the separation of finely dispersed particles of the strengthening phase of spherical shape and their coagulation occurs. At the same time, no noticeable change in the volumetric amount of the strengthening phase compared to the initial state (after HT) is observed. However, due to the presence of tantalum in the phases of the ЗМІ-11 alloy, phase transformations in its structure during prolonged thermal action at 950 °C proceed more slowly than in the N-155 alloy.

Metallographic analysis showed that in the structure of the N-155 and ЗМІ-11 alloys after prolonged thermal action on the basis of 5000 hours at temperatures of 850 °C and 950 °C, topological close-packed (TCP) phases, such as the σ- phase, were not detected, which indicates the stability of the solid solution of the alloys with respect to the release of harmful excess phases during prolonged thermal action.

Conclusions

1. Based on a comprehensive approach, a comparative analysis of alloys N-155 and ЗМІ-11 was carried out, which allows us to adequately predict the possibility of replacing the foreign alloy N-155 with the domestic ЗМІ-11.

2. It was established that during tests at 800 and 900 °C, the ultimate strength of alloy N-155 is 1.2 times lower than ЗМІ-11, and the long-term strength is 5.2 times lower, respectively.

3. It was shown that the amount of the strengthening phase in the ЗМІ-11 alloy is 6...10 % more, with a uniform distribution throughout the alloy body.

4. It was established that in the composition of the strengthening phase of the ЗМІ-11 alloy, the concentration of chromium, tungsten and molybdenum remains practically unchanged and does not depend on the presence of niobium. At the same time, in the composition of the strengthening phase of the ЗМІ-11 alloy, the concentration of cobalt increases by 1.4 times, and the concentration of aluminum and titanium decreases by 1.1 times compared to the N-155 alloy.

5. It was established that in the process of dissolving non-equilibrium eutectic precipitates, microvolumes arise, locally supersaturated with tungsten, chromium, titanium, in which the probability of formation of carbides on a more complex basis increases. It was established that in the process of prolonged thermal action, carbides on the basis of tantalum TaC and on a mixed basis (Ta, Ti)C in the ЗМІ-11 alloy are thermally more stable than carbides in the N-155 alloy.

References

1. Semiatin, S.L., Tiley, J.S., Zhang, F. et al. (2021). A Fast-Acting Method for Simulating Precipitation During Heat Treatment of Superalloy 718. Metall Mater Trans A 52, 483–499 https://doi.org/10.1007/s11661-020-06092-6

2. Sulzer, S., Hasselqvist, M., Murakami, H. et al. (2020). The Effects of Chemistry Variations in New Nickel-Based Superalloys for Industrial Gas Turbine Applications. Metall Mater Trans A 51, 4902–4921 https://doi.org/10.1007/s11661-020-05845-7

3. Xie, J., Ma, Y., Xing, W. (2019). Microstructure and mechanical properties of a new cast nickel-based superalloy K4750 joint produced by gas tungsten arc welding process. J Mater Sci, 54, 3558–3571. https://doi.org/10.1007/s10853-018-3081-y

4. Glotka O.A. 2020. Modelling the composition of carbides in nickel-based superalloys of directional. Journal of Achievements in Materials and Manufacturing Engineering, 102/1, 5–15. DOI: https://doi.org/10.5604/01.3001.0014.6324

5. Y.H. Kvasnytska, L.M. Ivaskevych, O.I. Balytskyi (2020). High-Temperature Salt Corrosion of a Heat-Resistant Nickel Alloy. Material Sciences, 56, 432–440. DOI: https://doi.org/10.1007/s11003-020-00447-5

6. P.G. Min, V.V. Sidorov, V.E. Vadeev (2020). Development of Corrosion and Heat-Resistant Nickel Alloys and their Production Technology with the Aim of Import Substitution. Power Technol Eng, 54, 225–231. DOI: https://doi.org/10.1007/s10749-020-01195-x

7. Hiroto Kitaguchi (2012). Microstructure-Property Relationship in Advanced Ni-Based Superalloys/ Hiroto Kitaguchi. – Open access peer-reviewed chapter, 210. https://doi.org/ 10.5772/52011

8. Zhao, GD., Yang, GL., Liu, F. et al. (2017). (2017). Transformation Mechanism of (γ + γ′) and the Effect of Cooling Rate on the Final Solidification of U720Li Alloy. Acta Metall. Sin. (Engl. Lett.) 30, 887–894 https://doi.org/10.1007/s40195-017-0566-7

9. Liang, T., Wang, L., Liu, Y. et al. (2020). Role of script MC carbides on the tensile behavior of laser-welded fusion zone in DZ125L/IN718 joints at 650 °C. J Mater Sci 55, 13389–13397 https://doi.org/10.1007/s10853-020-04931-w

10. Glotka, A.A. (2020). Distribution of Alloying Elements in the Structure of Heat-Resistant Nickel Alloys in Secondary Carbides / A.A. Glotka, S.V. Gaiduk // J Appl Spectrosc, 87, 812–819. DOI: https://doi.org/10.1007/s10812-020-01075-2

Одержано 10.03.2025

DOI 10.15588/1607-6885-2025-1-2

ПОРІВНЯЛЬНИЙ АНАЛІЗ КОМПЛЕКСУ ВЛАСТИВОСТЕЙ ЖАРОМІЦНИХ НІКЕЛЕВИХ СПЛАВІВ

Сергій Бєліков — д-р техн. наук, професор, професор кафедри транспортних технологій Національного університету «Запорізька політехніка», м. Запоріжжя, Україна, *e-mail: belikov@zp.edu.ua,* ORCID: 0000-0002-9510-8190

Віталій Кононов — канд. техн. наук, доцент, доцент кафедри деталей машин і підйомно-транспортних механізмів Національного університету «Запорізька політехніка», м. Запоріжжя, Україна, *e-mail; kononov1705@gmail.com,*ORCID: 0000-0002-0479-1386

Олександр Глотка — канд. техн. наук, доцент, доцент кафедри фізичного матеріалознавства Національного університету «Запорізька політехніка», м. Запоріжжя, Україна, *e-mail: glotka-alexander@ukr.net*,ORCID: 0000-0002-3117-2687

Михайло Сидоренко — канд. техн. наук, доцент, доцент кафедри деталей машин і підйомно-транспортних механізмів Національного університету «Запорізька політехніка», м. Запоріжжя, Україна, *e-mail: sidorenko.mik@gmail.com,* ORCID: 0000-0002-9097-9739

Сергій Пучек — аспірант кафедри транспортних технологій Національного університету «Запорізька політехніка», м. Запоріжжя, Україна, *e-mail: puchek777@gmail.com,* ORCID: 0009-0007-8077-6106

Мета роботи. *Провести порівняльні дослідження комплексу физико-механічних властивостей імпортного сплаву N-155 і вітчизняного сплаву ЗМІ-11 з метою збільшення ресурсу роботи лопаток, що обертаються. Провести порівняльні випробування на короткочасну і тривалу міцність сплавів в початковому стані (після термообробки), провести порівняльні випробування на короткочасну і тривалу міцність сплавів після тривалої теплової дії при Т = 850 ℃, 950 ℃ впродовж 1000, 3000, 5000 годин.*

Методи дослідження. *Зразки сплавів виготовляли зі зливків вагою 10 кг у вакуумній індукційній печі УППФ-3М в середовищі аргону при тиску 1,4–5,3 Па в тиглях з основним футеруванням з одночасною заливкою зразків рівновісної кристалізації. Хімічний аналіз проводили стандартними методами згідно з вимогами ТУ 14-1689-73 і ОСТ 1.90127-85. Дослідження мікроструктури проводили на мікрошліфах, площина яких орієнтована по нормалі до поверхні на світловому оптичному мікроскопі «Olympus IX-70» з цифровою відеокамерою «ExwaveHAD color video camera Digital Sony» при збільшеннях ×200, ×500, ×1000. Випробування міцності (ГОСТ 1497-61, ГОСТ 9651-61, ГОСТ 1497-84) проводили на стандартних циліндричних зразках (діаметр робочої частини 5мм, довжина 25мм) при температурах 200, 800, 900 і 1000 ℃ на розривній машині марки УМЭ-10ТМ. Випробування на тривалу міцність (ГОСТ 10145-81) проводили на стандартних циліндричних зразках при температурах 800, 900, 1000℃ і відповідних навантаженнях 600, 400, 180 МПа на машині АИМА-5-2.*

Отриманні результати. *Встановлено, що при випробуваннях 800 та 900℃ границя міцності сплаву N-155 в 1.2 рази нижча ніж ЗМІ-11, а довготривала міцність в 5.2 рази менша відповідно. Показано, що кількість зміцнюючої фази в сплаві ЗМІ-11 більше на 6…10 %, з рівномірним розподілом по тілу сплаву. Встановлено, що у складі зміцнюючої фази сплаву ЗМІ-11 концентрація хрому, вольфраму і молібдену залишається практично незмінною і не залежить від наявності ніобію. В той же час, у складі зміцнюючої фази сплаву ЗМІ-11 підвищується концентрація кобальту в 1,4 разу і знижується в 1,1 разу концентрація алюмінію і титану в порівнянні із сплавом N-155. Встановлено, що в процесі розчинення нерівноважних евтектичних виділень виникають мікрооб'єми, локально пересичені вольфрамом, хромом, титаном, в яких підвищується вірогідність утворення карбідів на складнішій основі. В ході досліджень було встановлено, що в процесі тривалої теплової дії карбіди на основі танталу TaC і на змішаній основі (Ta, Ti) C в сплаві ЗМІ-11 термічно стабільніші, ніж карбіди в сплаві N-155.*

Наукова новизна. *Отримані результати дають змогу зрозуміти термодинаміку процесів фазоутворення в двох системах легування та встановити залежності між легуючими елементами та фазовим складом сплаву.*

Практична цінність. *Отримані результати дають змогу рекомендувати як замінника закордонним N-155 на вітчизняний ЗМІ- 11 без втрати властивостей та ресурсу експлуатації.*

Ключові слова: *жароміцні нікелеві сплави, фазовий склад, розподіл легувальних елементів, жароміцність, карбіди.*

DOI 10.15588/1607-6885-2025-1-2

Список літератури

1. A Fast-Acting Method for Simulating Precipitation During Heat Treatment of Superalloy 718 / Semiatin, S.L., Tiley, J.S., Zhang, F. et al. // Metall Mater Trans A. – 2021. – N 5. – P. 483–499. https://doi.org/10.1007/s11661-020-06092-6.

2. The Effects of Chemistry Variations in New Nickel-Based Superalloys for Industrial Gas Turbine Applications / Sulzer, S., Hasselqvist, M., Murakami, H. et al. // Metall Mater Trans. – 2020. – A 51, P. 4902–4921. https://doi.org/10.1007/s11661-020-05845-7.

3. Xie, J. Microstructure and mechanical properties of a new cast nickel-based superalloy K4750 joint produced by gas tungsten arc welding process / Xie, J., Ma, Y., Xing, W. // J Mater Sci. – 2019. – N 54. – P. 3558–3571. https://doi.org/10.1007/s10853-018-3081-y.

4. Glotka O.A. Modelling the composition of carbides in nickel-based superalloys of directional crystallization / Glotka O.A. // Journal of Achievements in Materials and Manufacturing Engineering. – 2020. – 102/1 – P. 5–15. doi:10.5604/01.3001.0014.6324.

5. Kvasnytska, Y.H. High-Temperature Salt Corrosion of a Heat-Resistant Nickel Alloy / Kvasnytska, Y.H., Ivaskevych, L.M., Balytskyi, O.I. // Mater Sci. – 2020. – N 56. – P. 432–440. doi: 10.1007/s11003-020-00447-5.

6. Min, P.G. Development of Corrosion and Heat-Resistant Nickel Alloys and their Production Technology with the Aim of Import Substitution / Min, P.G., Sidorov, V.V., Vadeev, V.E. // Power Technol Eng. – 2020. – N 54. – P. 225–231. doi: 10.1007/s10749-020-01195-x.

7. Hiroto Kitaguchi Microstructure-Property Relationship in Advanced Ni-Based Superalloys/ Hiroto Kitaguchi // Open access peer-reviewed chapter. – 2012. – P. 210. https://doi.org/ 10.5772/52011.

8. Transformation Mechanism of ($\gamma + \gamma'$) and the Effect of Cooling Rate on the Final Solidification of U720Li Alloy / Zhao, GD., Yang, GL., Liu, F. et al. //Acta Metall. Sin. (Engl. Lett.). – 2017. – N 30. – P. 887–894. https://doi.org/10.1007/s40195-017-0566-7.

9. Role of script MC carbides on the tensile behavior of laser-welded fusion zone in DZ125L/IN718 joints at 650 °C / Liang, T., Wang, L., Liu, Y. et al. // J Mater Sci. – 2020. – P. 55, 13389–13397. – https://doi.org/10.1007/s10853-020-04931-w.

10. Glotka, A.A. Distribution of Alloying Elements in the Structure of Heat-Resistant Nickel Alloys in Secondary Carbides / Glotka, A.A., Gaiduk, S.V. // J Appl Spectrosc. – 2020. – N 87. – P. 812–819. doi: 10.1007/s10812-020-01075-2.

DOI 10.15588/1607-6885-2025-1-2